Published in final edited form as:
Bone. 2013 August ; 55(2): 277–287. doi:10.1016/j.bone.2013.04.001.

Constitutive protein kinase A activity in osteocytes and late osteoblasts produces an anabolic effect on bone

Richard S. Kao, **Marcia J. Abbott**, **Alyssa Louie**, **Dylan O'Carroll**, **Weidar Lu**, and **Robert Nissenson***
University of California San Francisco, San Francisco, CA, USA Veterans Affairs Medical Center, San Francisco, CA, USA

Abstract

Osteocytes have been implicated in the control of bone formation. However, the signal transduction pathways that regulate the biological function of osteocytes are poorly defined. Limited evidence suggests an important role for the G_s/cAMP pathway in osteocyte function. In the present study, we explored the hypothesis that cAMP-dependent kinase A (PKA) activation in osteocytes plays a key role in controlling skeletal homeostasis. To test this hypothesis, we mated mice harboring a Cre-conditional, mutated PKA catalytic subunit allele that encodes a constitutively active form of PKA (CαR) with mice expressing Cre under the control of the osteocyte-specific promoter, DMP1. This allowed us to direct the expression of CαR to osteocytes in double transgenic progeny. Examination of Cre expression indicated that CαR was also expressed in late osteoblasts. Cortical and trabecular bone parameters from 12-week old mice were determined by μCT. Expression of CαR in osteocytes and late osteoblasts altered the shape of cortical bone proximal to the tibia-fibular junction (TFJ) and produced a significant increase in its size. In trabecular bone of the distal femur, fractional bone volume, trabecular number, and trabecular thickness were increased. These increases were partially the results of increased bone formation rates (BFRs) on the endosteal surface of the cortical bone proximal to the TFJ as well as increased BFR on the trabecular bone surface of the distal femur. Mice expressing CαR displayed a marked increase in the expression of osteoblast markers such as osterix, runx2, collagen 1α1, and alkaline phosphatase (ALP). Interestingly, expression of osteocyte marker gene, DMP1, was significantly up-regulated but the osteocyte number per bone area was not altered. Expression of SOST, a presumed target for PKA signaling in osteocytes, was significantly down-regulated in females. Importantly, no changes in bone resorption were detected. In summary, constitutive PKA signaling in osteocytes and late osteoblasts led to a small expansion of the size of the cortical bone proximal to the TFJ and an increase in trabecular bone in female mice. This was associated with down-regulation of SOST and up-regulation of several osteoblast marker genes. Activation of the PKA pathway in osteocytes and late osteoblasts is sufficient for the initiation of an anabolic skeletal response.

Keywords

Osteocyte; Protein kinase A; Cyclic AMP; Dentin matrix protein 1

*Corresponding author at: University of California San Francisco, San Francisco, CA, USA. Fax: 415-750-6929. robert.nissenson@ucsf.edu. .

Supplementary data to this article can be found online at http://dx.doi.org/10.1016/j.bone.2013.04.001.

Introduction

Maintenance of bone quality is critical for the skeleton to provide physical support. This is accomplished by continuous bone remodeling performed by bone-resorbing cells, osteoclasts, and bone forming cells, osteoblasts, at the bone surface. The interior of bone consists of mineralized matrix and osteocytes. Importantly, osteocytes are the most abundant cell type in bone and have a unique three-dimensional distribution within the bone tissue. Little is known about the function of osteocytes due to their inaccessible physical location. They are thought to perform multiple functions. Their long dendrite-like processes may facilitate long distance cell–cell communication, so they are potentially capable of acting as mechanosensors of the bone. Moreover, the osteocyte network represents an enormous surface area for ready access to matrix minerals. Osteocytes secrete factors such as dentin matrix protein 1 (DMP1), PHEX, MEPE, and FGF23 that can regulate systemic mineral homeostasis [1–3], which in turn affects bone remodeling. Finally, osteocytes may exert paracrine effects on neighboring bone cells to regulate bone modeling and remodeling. For example, osteocyte-like cells in culture have been shown to support osteoclast formation and activation [4] as well as inhibiting osteoclastic bone resorption function [5]. Osteocytes secrete sclerostin, a protein that produces inhibitory effects on bone formation presumably though paracrine suppression of Wnt signaling in osteoblast lineage cells [6]. In addition, conditioned medium from osteocyte-like cells in culture can stimulate the differentiation of bone marrow mesenchymal stem cells into osteoblasts by a mechanism that is not well defined [7].

Parathyroid hormone (PTH) is a key regulator of calcium homeostasis and plays an important role in the control of bone remodeling. It is secreted by the parathyroid glands in response to changes in serum calcium concentration. The principal target organs for PTH are the kidney and the skeleton. It has dual effects on bone formation depending on the pattern and duration of the elevated circulating concentration of PTH. Continuous high levels of PTH, as in the case of renal failure, promote bone resorption. On the other hand, intermittent exposure to exogenous PTH stimulates bone formation. Although the molecular mechanism underlying this phenomenon is not clear, G protein signaling via PTH/PTH related protein receptor (PTH1R) is involved.

Several extracellular regulators of skeletal function are known to exert their actions through G protein-coupled receptors (GPCRs) that are expressed in the osteoblast membrane. The best-studied GPCR that regulates skeletal function is PTH1R [8]. This receptor is coupled to at least two G proteins, G_s and G_q, resulting in the activation of diverse downstream effectors [9–12]. In G_s-mediated signaling, activation of G_s by a ligand-bound GPCR leads to increased production of the second messenger cAMP from ATP by adenylate cyclase. Activation of G_i, on the other hand, inhibits the production of cAMP from ATP. Conditional deletion of the α subunit of G_s in osteoblast lineage cells resulted in reduced trabecular bone formation [13]. Targeted expression in osteoblasts of constitutively active, G_s-coupled GPCRs resulted in markedly increased trabecular bone mass [14,15], whereas expression of a constitutively-active G_i-coupled receptor in osteoblasts produced trabecular osteopenia [16]. Moreover, blockade of G_i signaling in osteoblasts by pertussis toxin produced increases in cortical and trabecular bones [17]. These findings highlight the importance of the G_s/cAMP pathway in promoting bone formation and in mediating the anabolic response of the skeleton to PTH.

Elevated cellular levels of cAMP can act through multiple mechanisms. The most common mechanism is via activation of a pool of dormant PKA. PKA is a multi-subunit enzyme consisting of two regulatory and two catalytic subunits. Binding of cAMP to the regulatory subunits causes conformational changes leading to dissociation of regulatory subunits from

the catalytic subunits, thereby relieving the inhibitory effect on the catalytic subunits. In some cases, cAMP can directly regulate membrane ion channels without participation by PKA [18], although this has not been demonstrated in osteoblast-lineage cells. Finally, cAMP has been shown to activate GTP exchange proteins for the small GTPases Rap1 and Rap2 (termed “Epacs”) by a PKA-independent mechanism [19,20]. Indeed, there is evidence that PTH1R signaling utilizes the Epac pathway in osteoblastic cells [21], although the physiological relevance of this is unclear.

Osteocytes, being terminally differentiated osteoblasts, not surprisingly also express PTH1R [22]. Increased cAMP in osteocytes after exogenous PTH administration had been demonstrated in vivo [22,23]. Accumulation of cAMP in response to PTH in purified osteocytes and clonal osteocytic cell lines demonstrated the existence of PTH1R on osteocytes and the coupling of cAMP/PKA pathway to PTH signaling [24–28]. Intermittent administration of PTH can elevate intracellular concentration of cAMP in osteocytes and is accompanied by an increased osteocyte density [29]. Finally, expression of constitutively active PTH1R in osteocytes showed a dramatic increase in bone mass in mice, whereas targeted ablation of PTH1R in osteocytes led to mild osteopenia in mice [30,31]. Activation of PTH1R in osteocytes by PTH is known to amplify the osteogenic response to mechanical loading in vivo [32–35] and reduce immobilization-induced bone loss [36,37], indicating an important role of PTH in regulating signal transduction induced by loading in osteocytes. Thus, osteocytes could be another target of PTH to exert its anabolic skeletal effect. This may be accomplished by suppressing osteocyte apoptosis [27] or down-regulation of an osteocyte-specific signal, sclerostin, which inhibits proliferation and maturation of osteoblast [38,39] and stimulates osteoblast apoptosis via canonical Wnt signaling pathway [6].

Another GPCR expressed by osteocytes is the prostaglandin E2 (PGE_2) receptor [40]. Mechanical forces stimulate secretion of PGE_2 by bone cells including osteocytes [41], and binding of PGE_2 to its cognate GPCR also activates cAMP/PKA pathway [40]. Thus, both PTH signaling and mechanically stimulated PGE_2 signaling converge on the cAMP/PKA pathway. This may explain the additive anabolic effect of PTH on mechanically stimulated bone growth. Moreover, other extracellular signals can activate as yet unidentified GPCRs that are coupled to the cAMP/PKA pathway.

Mutations in the gene encoding for PKA regulatory subunit 1A are the basis of two human diseases, Carney complex and primary pigmented nodular adrenocortical disease [42], and additionally, enhanced expression of RIα is associated with cancer genesis, indicating the importance of this kinase in cellular functions [43,44]. Although there is considerable information available concerning the effects of cAMP/PKA signaling in osteoblasts, the role of this signaling pathway in osteocytes in contributing to skeletal homeostasis is not known. Although a few osteocytic cell lines have been established [45,46] and methods of isolating primary osteocytes have been refined, cultured osteocytes on a dish cannot completely mimic their counterpart in their natural environment. Thus, the precise role of this signaling pathway in osteocytes for mediating skeletal development and skeletal response to anabolic regimen of PTH needs to be addressed in an animal model.

DMP1 is a secreted matrix protein that functions to promote mineralization and is highly expressed in osteocytes and odontoblasts [2,47,48]. Because of its specific expression in osteocytes, promoter driving its expression has been used to drive expression of a transgene specifically in osteocytes [49]. Here we report the use 10-kb DMP1 promoter to drive expression of Cre recombinase to permit expression of the Cre-inducible transgene CαR in osteocytes and the impact of constitutively elevated PKA signaling in osteocytes in skeletal development.

Material and methods

Animals

Mice harboring one copy of Cre-inducible CαR mutation were the gift of Dr. Stanley McKnight at University of Washington and have been previously described [50]. Mice harboring Cre recombinase under the control of the 10-kb DMP1 promoter were the gift of Dr. Lynda Bonewald at University of Missouri-Kansas City [49]. We targeted the expression of CαR to osteocytes by crossing mice heterozygous for Cre-inducible CαR with mice heterozygous for 10-kb DMP1 promoter driving the expression of Cre to obtain double transgenic DMP1Cre,CαR progeny. Mice were maintained on a C57BL/6 background for at least six generations and fed with standard mouse chow. Littermate wild-type, single transgenic CαR, and single transgenic DMP1Cre mice were analyzed for skeletal phenotypes as controls. Tibiae, femurs, sera, and RNA isolated for analysis were derived from 3-month old mice. All transgenic mouse studies were approved by and performed in accordance with the Institutional Animal Care and Use Committee at the Veterans Affairs Medical Center, San Francisco.

Genotyping

Mouse tail genomic DNA was extracted using a REDExtract-N-Amp Tissue PCR Kit (Sigma-Aldrich, St. Louis, MO). The CαR transgene was identified using the primers 5′-GCA GCC CTT CTC TCT ACC AA-3′ and 5′-GGT CCC ACA CAA GGT ACG C-3′, resulting in a fragment just over 100-bp in length. The presence of the Cre transgene was determined using the primers 5′-CAT TTG GGC CAG CTA AAC AT-3′ and 5′-TGC ATG ATC TCC GGT ATT GA-3′, producing a 662-bp fragment. PCR was performed with the following cycling profile: 94 °C for 1.5 min; 35 cycles of 94 °C for 30 s, 60 °C for 1 min, and 72 °C for 1.5 min.

Microcomputed tomography (μCT)

Left femurs and tibiae from 3-month old mice were isolated and cleaned of adherent tissue. Before μCT analysis, bones were fixed for 1 to 2 days in 10% neutral buffered formalin (NBF; FisherScientific, Pittsburgh, PA, USA) and dehydrated in 70% ethanol. The bones were imaged using a VivaCT-40 μCT system (Scanco Medical AG, Bruttisellen, Switzerland). All images were obtained using an X-ray energy of 55 kV with a voxel size of 10.5 μm and integration time of 1000 ms. Left distal femoral metaphysis was scanned in a region consisted of 100 serial cross-sections (1.02 mm beginning at the bottom of metaphyseal growth plate and extending into the shaft proximally). The trabecular bone of the distal femur was assessed using a global thresholding protocol with segmentation values of 0.4/1/270. To assess cortical bone, left tibia diaphysis was scanned in a region consisted of 40 serial cross-sections (0.42 mm) immediately below TFJ proximally, using a global thresholding protocol with segmentation values of 0.8/1/365.

Histomorphometry

Mice were injected with 20 mg/kg of calcein (Sigma-Aldrich, St. Louis, MO, USA) 30 and 7 days before euthanasia and with 15 mg/kg of demeclocycline (Sigma-Aldrich) 2 days before euthanasia. Mice were euthanized at 3-month of age, and tibiae and femurs were isolated, fixed in 10% NBF, and stored in 70% ethanol. Following μCT analysis, the undecalcified bone samples were embedded in methyl methacrylate and sectioned with Leica RM 2255 and 2265 microtomes (Leica, Bannockburn, IL, USA). Assessment of cortical bones was performed on 10-μm transverse sections in the region proximal to TFJ. Trabecular bone in the distal femur was assessed in an irregular region of interest defined by four boundaries: a line traced at a distance of 500 μm from the growth plate, two lines drawn parallel to the

cortical bone at a distance of 500 μm from the endocortical surface, and a straight line drawn perpendicular to the bone at a distance of 1.0 mm from the lowest point of the growth plate. An average of 1.6 mm^2 of trabecular bone tissue (including marrow) was measured. To measure the number of osteoclast per bone surface in the trabecular bone, 5-μm longitudinal sections from the distal femur were stained for tartrate resistant acid phosphatase (TRAP). Hematoxylin and eosin were used to stain the same sections to measure trabecular bone osteocyte number per bone area in the secondary spongiosa. Osteocytes in the cortex surrounding the secondary spongiosa were measured to determine cortical bone osteocyte number per bone area. Mosaic-tiled images were acquired at 200× magnification with a Zeiss Axioplan Imager M1 microscope (Carl Zeiss MicroImaging, Thornwood, NY, USA) fitted with a motorized stage. The tiled images were stitched and converted to a single image using the Axiovision software (Carl Zeiss MicroImaging) prior to blinded analyses being performed using image-analysis software (Bioquant Image Analysis Corp., Nashville, TN, USA). The dynamic indices of bone formation that were measured include percent mineralizing surface (MS), mineral apposition rate (MAR), and surface-based bone-formation rate (BFR/BS).

RNA extraction and real-time PCR

Right femurs and tibiae were isolated and cleaned of adherent tissue. The marrow elements were flushed out leaving only the bone tissue. Frozen tissues were pulverized using a bio-pulverizer (Biospec Products Inc., Bartlesville, OK), followed by RNA extraction using RNA-STAT60 (Ted-Test Inc.). RNA was purified using a Micro-to-Midi Total RNA Purification Kit (catalog no. 12183-018; Invitrogen; Carlsbad, CA). A second step of purification was carried out using a RNeasy Mini Kit (Qiagen Cat. #74104). Reverse transcription was carried out using TaqMan Reverse Transcription Reagents (Applied Biosystems Part# N808-0234). Primers were synthesized by Elim Biopharmaceuticals, Inc. or Applied Biosystems (TaqMan Gene Expression Assay). SYBR Green I-based (Applied Biosystems; part no. 4309155) and TaqMan-based gene amplifications were measured using the ABI Prism 7900HT real-time thermocycler. Analysis was carried out using 7300 System SDS version 1.4 software supplied with the machine. Runx2, osterix, and ALP expression were normalized to L19 because the Ct number of these genes was closer to L19 Ct number. Collagen 1α1 and osteocalcin were normalized to GAPDH.

Serum chemistry

Blood samples were obtained from mice at the time of euthanasia. Quantitative determination of N-terminal propeptide type 1 procollagen (P1NP) in the serum was carried out using Rat/Mouse PINP EIA (cat #AC-33 F1, Immunodiagnostic Systems). Quantitation of pyridinoline (PYD) was carried out using MicroVue Serum PYD (cat # 8019, Quidel Corporation). Serum alkaline phosphatase was quantified using an Ace Alera Clinical Chemistry Analyzer (Alfa Wassermann Technologies).

Immunohistochemistry

Calvaria was isolated and fixed in neutral buffered formalin and decalcified in 10% Tris–ethylenediaminetetraacetic acid (EDTA) for approximately two weeks. Decalcified calvaria was embedded in paraffin and sectioned at 5 micron-thickness. Sections were de-paraffinized with xylenes (3 × 3 min) followed by 1:1 xylene:100% ethanol (ETOH) for 3 min, 100% ETOH 2 × 3 min, 95% ETOH 3 min, 70% 3 min, 50% 3 min and running tap water. Antigen retrieval was performed with sodium citrate (pH 6) at 37 °C for 20 min. Endogenous peroxidases were blocked using 3% hydrogen peroxide for 10 min followed by a 10 min incubation with 0.1% Tween-PBS. Slides were blocked with 1% BSA in PBS followed by an overnight incubation with anti-Cre (Abcam, #ab24606) primary antibody (1:500) at 4 °C. A secondary immunohistochemistry HRP/DAB (Millipore, #DAB150) kit

was used according to the manufacturer's protocol. Briefly, sections were rinsed with 0.1% Tween-PBS followed by 10 min incubation with streptavidin HFP, 10 min in DAB/ chromogen reagent, and 1 min in hematoxylin counter stain.

Statistical analysis

Data are presented as mean ± SEM. Statistical significance was determined using a paired *t* test between double transgenic animals and sex-matched DMP1Cre single transgenic controls. To determine statistical differences among wild-type, CαR single transgenic, DMP1Cre single transgenic, and double transgenic mice, 1-way ANOVA and Bonferroni all pairs post-hoc method was used. GraphPad Prism 5 software was used for all statistical calculations, and significance was set at a p value of <0.05.

Results

CαR transcripts are expressed in long bones of DMP1Cre,CαR mice

New genetic tools are now available in mouse to study the function of PKA in vivo. A constitutively active form of PKA has been identified [51]. In mice, there are two genes encoding for PKA catalytic subunits (Cα and Cβ) and four isoforms of regulatory subunits exist (RIα, RIβ, RIIα, and RIIβ). Expression of different subunits is tissue-specific but the expression of the α subunits is widespread [52]. The constitutively active form of mutant, CαR, is the result of conversion of tryptophan 196 to arginine in Cα. This mutation prevents effective inhibition of the catalytic subunits by the regulatory subunits under normal cellular concentrations of cAMP, without perturbing the normal catalytic function of CαR [50,53]. Consequently, there is an enhanced dissociation of CαR from the regulatory subunits in the presence of low levels of cAMP. At the same time, the maximal catalytic activity was not changed [51].

To determine whether PKA signaling in osteocytes is important for skeletal homeostasis, double transgenic DMP1Cre,CαR mice were generated from the cross between mice harboring Cre recombinase under the control of 10-kb dentin matrix protein 1 (DMP1) promoter and mice heterozygous for Cre-inducible CαR. This promoter directs osteocytes-specific expression of transgene in mice [2,47]. The CαR allele carries a floxed intronic neomycin cassette (flanked by two loxP sites) that interferes with the production of full-length mutant CαR mRNA in cells harboring CαR (Fig. 1A). This mutation, which resides in exon 7, was detected only in RNA extracted from femurs and tibiae of DMP1Cre,CαR mice (Fig. 1B).We further tested the Cre dependency of the CαR expression. Bone marrow stromal cells were isolated from mice heterozygous for Cre-inducible CαR transgene and infected with adenovirus containing a functional copy of Cre gene or adenovirus containing an empty vector as control. Only cells expressing Cre produced the predicted CαR transcript (data not shown).

DMP1 promoter drives expression of Cre recombinase in osteocytes as well as late stage osteoblasts

To determine that 10-kb DMP1 promoter actually drives the expression of Cre in osteocytes, we examined expression of the Cre protein in calvaria. Immunohistochemistry detected Cre expression in a large portion of osteocytes in the single transgenic DMP1Cre (Fig. 2B) but not in the wild-type calvaria (Fig. 2A). However, these results did not exclude the possibility that Cre expression took place in other cell types, such as late stage osteoblasts, since we also detected positive staining in those cells as others have previously shown [49,54].

Mice expressing the constitutively active form of PKA in osteocytes and late osteoblasts exhibit altered bone shape and higher bone mass

DMP1Cre,CαR mice were fertile, exhibited normal size and weight (data not shown). Micro-CT three-dimensional reconstruction of the cortical bone proximal to TFJ in 3-month old mice showed altered cortical bone shape. The anterior-medial and posterior-lateral sides of cortical bone exhibited concave bone surfaces in majority of double transgenic animals as viewed transversely (Fig. 3A). Micro-CT analysis showed increased tissue volume in DMP1Cre,CαR mice as compared to wild-type, single transgenic CαR, and single transgenic DMP1Cre controls (Fig. 3B). Bone volume also increased when compared to the wild-type and single transgenic CαR controls (Fig. 3B). However, fractional bone volume and cortical thickness were not changed (Fig. 3B). Histomorphometric measurement of periosteal and endocortical bone surface perimeters confirmed the expansion of the circumference of the cortical bone proximal to TFJ (Fig. 3C). Periosteal and endosteal bone surfaces were expanded by 8% and 21%, respectively, as compared to the DMP1Cre control. Micro-CT of the distal femurs showed high trabecular bone mass. Fractional bone volume, trabecular number, and trabecular thickness were significantly greater than all other genotypes (Fig. 3D). These results were confirmed by static histomorphometric measures (data not shown). Thus, constitutive active PKA signaling in osteocytes and late osteoblasts resulted in an increase in bone mass.

Constitutively active PKA signaling in osteocytes and late osteoblasts leads to increased bone formation

To determine whether the changes in the geometry of cortical bone proximal to TFJ and the increase in trabecular bone in the distal femur were associated with an increase in bone formation, dynamic histomorphometry was carried on bone surfaces of these regions. On the periosteal bone surface of DMP1Cre,CαR mice, MAR was increased by 69%, as compared to the DMP1Cre control (Fig. 4A). On the endosteal bone surface, MAR and BFR/BS increased by 95% and 127%, respectively, in the double transgenic animals (Fig. 4A). Moreover, the percent mineralized surface on the endosteal surface was increased by nearly 20% (Fig. 4A). Dynamic histomorphometric measurement of trabecular bone in the distal femur demonstrated increased MAR and BFR/BS on the trabecular bone surface of DMP1Cre,CαR mice (Fig. 4B). Circulating levels of bone formation markers, P1NP and ALP, confirmed the increased bone formation detected by histomorphometry. Serum levels of P1NP showed a trend of increase while serum levels of ALP were significantly higher in DMP1Cre,CαR mice as compared to single transgenic CαR or DMP1Cre controls (Fig. 4C).

DMP1Cre,CαR mice do not exhibit evidence of elevated bone resorption

Since we observed increased bone formation in DMP1Cre,CαR mice, we evaluated whether this increase in bone formation was accompanied by an increased bone turnover. A serum marker of bone resorption, PYD, was measured and showed no difference as compared to other genotypes (Fig. 5A). Osteocytes are known to have a role in systematic mineral homeostasis. Thus, we also measured the serum levels of calcium and phosphate but found them to be unaffected by genotype (data not shown). Quantitation by real-time PCR of mRNA levels of RANKL and OPG in the long bone RNA showed no significant changes in the ratio of RANKL:OPG gene expression in DMP1Cre,CαR mice (Fig. 5B). Finally, histomorphometric measurement of the number of osteoclasts on the trabecular bone surface of distal femurs showed a 34% reduction in the number of osteoclast per bone surface as compared to DMP1Cre controls (Fig. 5C). Interestingly, the total number of osteoclast per tissue volume was not changed (data not shown).

Constitutively active PKA signaling in osteocytes does not change osteocyte number but up-regulates DMP1 transcript levels in long bones

We next examined the direct effects of targeting CαR expression to osteocytes on osteocytes themselves. Histomorphometric quantification of osteocyte in cortical and trabecular bones of distal femurs revealed no changes in osteocyte number per bone area (osteocyte density) (Fig. 6A). We then quantified by real-time PCR the expression level of osteocyte-specific genes, such as DMP1 and SOST, in the long bone. Interestingly, DMP1 transcript levels were up-regulated in DMP1Cre,CαR mice as compared to DMP1Cre controls (Fig. 6B). On the other hand, expression of SOST was modestly down-regulated by constitutively active PKA signaling in osteocytes in females (Fig. 7B).

Osteoblast differentiation marker genes are up-regulated while SOST expression is down-regulated

Increased MAR and BFR in DMP1Cre,CαR mice were indicative of increased bone formation. Therefore, we sought to determine the effect of constitutively active PKA in osteocytes and late osteoblasts on osteoblast maturation. Long bones from DMP1Cre,CαR mice exhibited increased expression of several genes that are associated with osteoblast differentiation, suggesting increased osteoblast differentiation (Fig. 7A). Wnt/β-catenin pathway plays an important role in normal bone biology, and deregulation of this process contributes to bone diseases [55–57]. To determine whether PKA signaling in osteocytes and late osteoblasts could affect Wnt/β-catenin pathway in cells of osteoblast lineage, we measured transcript levels of Wnt/β-catenin pathway modulators regulated by PTH/cAMP signaling. We also measured the expression levels of canonical Wnt pathway target genes in long bones. Transcript levels of Dkk1 in the long bone were not affected by constitutively active PKA in osteocytes and late osteoblasts (Fig. 7B). As mentioned previously, SOST expression was significantly down-regulated by constitutively active PKA (Fig. 7B). In accordance with the result of the lower SOST expression, transcript levels of Wnt target genes, Axin2 and Tcf1/7, were up-regulated (Fig. 7C). More importantly, increased Axin2 protein expression was detected by immunohistochemistry in the calvarial osteocytes, although an increase was also detected in osteoblasts and some unidentified marrow cells (Supplemental Fig. 3). These results are consistent with the notion that PKA signaling in osteocytes and late osteoblasts depresses Wnt signaling in osteoblast-lineage cells at least in part through down-regulation of SOST.

Discussion

While the effects of PTH1R activation in osteoblasts have been intensely studied, the effects of activation of PTH1R and its downstream signal transducers in osteocytes are not well known. Recent findings on the impact of the expression of a constitutively active PTH1 receptor in osteocytes in mice as well as a mouse model of inducible targeted ablation of PTH1R in osteocytes revealed an important role of PTH1R signaling in osteocytes on skeletal homeostasis [30,31,58]. To shed some light on the contribution of different signaling pathways that can be activated by PTH1R or other GPCRs, we focused on the function of one key signaling mediator of GPCR signaling, PKA.

In vivo osteocyte and late osteoblast PKA activity was modulated by the introduction of a mutated PKA catalytic subunit, which is less sensitive to regulation [50,53], resulting in high basal PKA activities. The resulting skeletal phenotypes included an expansion of the size and an alteration in the shape of the cortex proximal to the TFJ. Increased BFR on the periosteal surface and MAR on the endosteal surface partially explained the enlargement of the periosteal and endocortical perimeters. Elevated PKA activity in osteocytes and late osteoblasts also led to increased BFR on trabecular bone surfaces leading to increased

trabecular bone and trabecular numbers in the distal femurs of female mice. These increases in bone formation in both cortical and trabecular bones were not accompanied by concomitant increases in bone resorption. Serum levels of pyridinoline and the ratio of RANKL:OPG gene expressions were not changed. In fact, the number of osteoclasts per bone surface in trabecular bone was reduced, suggesting decoupling of bone turnover from bone formation. In this case, the number of osteoblast relative to the number of osteoclast within the BMU could be altered since osteoblast number per bone surface remained the same (data not shown), resulting in bone formation outpacing bone resorption.

This lack of alteration in bone resorption is in stark contrast to the bone turnover phenotypes in mice expressing constitutively active PTH1R in osteocytes. In that mouse model, there was an increase in the numbers of osteoblasts and osteoclasts, resulting in high rates of bone remodeling [30,58]. In addition, our model did not exhibit increased thickness in the cortex nor increased cortical porosity. However, the two mouse models did exhibit some similarities including increased trabecular bone mass, increased gene expression of osteoblast marker genes, increased BFR on the periosteal surface, and suppression of SOST expression [30,58]. PTH1R signaling can activate additional signal mediators such as arrestin, G_q, Epacs, and cAMP-gated ion channels, which act upstream of PKA [9–12,18–21]. High bone remodeling observed in mice expressing constitutively active PTH1R in osteocytes might require the activation of one or more of these signaling pathways. Activation of PKA pathway alone may not be sufficient to trigger higher bone remodeling. Alternatively, the constitutively active PTH1R may activate PKA signaling in osteocytes to a higher degree than that produced by CαR. In mice expressing CαR in hepatocytes, CαR from liver extracts is actually less responsive to exogenous cAMP stimulation than the wild-type Cα [51]. PKA signaling that is more responsive to PTH or other upstream signals may be required to stimulate bone remodeling. Altogether, the high basal catalytic activities of CαR in osteocytes and late osteoblasts did not produce detectable increases in bone resorption.

Skeletal analyses of TFJ and distal femurs of male mice expressing the CαR allele in osteocytes and late osteoblasts also showed increased anabolic responses, although the increase in bone mass was not as evident as in females, particularly in the trabecular bone of the distal femur (Supplemental Fig. 1). No expansion of the size of the cortex was detected but the shape of the cortex was altered in the same fashion (Supplemental Fig. 1). Mechanotransduction by osteocytes may be altered by the elevated PKA activity, leading to changes in the shape of cortex. It is also possible that the quality of bone may be affected by PKA signaling, and the tibia may compensate by remodeling the shape of the cortex to support mechanical loading. The phenotypic differences between the two sexes appeared to be mainly confined to the degree of increase in bone mass. The basis for this difference is not clear, but it is noteworthy that constitutive PKA signaling suppressed SOST expression in females but not in males (Supplemental Fig. 2). Interestingly, without SOST suppression, male mice expressing CαR in osteocytes and late osteoblasts still exhibited increased bone forming activities (Supplemental Table 1 and Fig. 2). Regulation of SOST expression may not be the only mechanism through which PKA signaling could control Wnt/β-catenin pathway. PKA can potentially control the protein levels of β-catenin through multiple mechanisms [59,60]. Further studies are warranted to examine the molecular basis for the gender difference in sensitivity of the SOST gene in osteocytes to down-regulation by PKA.

It’s well established that PTH can suppress sclerostin expression to increase bone mass, our data suggests that activation of PKA pathway alone in osteocytes can reduce the gene expression of SOST [38,39,61]. Strong evidence has shown the requirement of PTH1R in osteocytes to suppress sclerostin expression by osteocytes [30,62,63]. However, hormonal signal is not the only activator of PKA pathway in osteocytes to exert skeletal effects.

Sclerostin expression can also be regulated by mechanical stimuli, such as loading and unloading [64–66]. The role of Wnt signaling in adaptive response of skeleton was noticed early on when mice expressing LRP5 receptor with G171V mutation exhibited particularly high bone density in the weight-bearing areas [67]. Recent evidence indicates that osteocyte-like MLO-Y4 cells can also respond to mechanical stress to produce PGE_2 and activate cAMP/PKA pathway [40,68]. Whether osteocytes can utilize the same signaling pathways activated in osteoblast to produce skeletal responses remains to be investigated. Nevertheless, our results reinforce the idea that hormonal signal such as PTH, mechanical signal transduced byPGE_2, and other stimulatory G protein-coupled GPCRs could signal through PKA in osteocytes to control bone formation.

The effects of constitutively active PKA activity in osteocytes were mostly assessed indirectly by examining skeletal changes. Reduction in the gene expression of SOST was one of the indicators of the direct effect of modulated PKA signaling on osteocytes. Detection for DMP1 gene expression demonstrated increased transcript levels in the long bones of mice expressing constitutively active form PKA in osteocytes and late osteoblasts. High transcript levels may imply an up-regulation of gene expression on a per cell basis. Alternatively, the proportion of DMP1-positive cells among the total cell population could have increased. To explore the latter possibility, we counted the number of osteocytes within both cortical and trabecular bones of the distal femur and found no changes in osteocyte density. Changes in osteocyte density in other regions of the long bone cannot be excluded. Intermittent administration of PTH has been shown to increase osteocyte survival [27]. However, mice expressing constitutively active PTH1R in osteocytes exhibited no changes in osteocyte apoptosis [30]. Whether PKA activation in osteocytes can reduce osteocyte apoptosis remains to be seen.

Although attempts were made to determine the specific expression of CαR in osteocytes by examining Cre protein expression in histological sections, we failed to rule out the possibility that the mature osteoblast DMP1 could also drive the expression of CαR. Osteoblast CαR signaling probably contributed in part to skeletal, cellular, molecular, and biochemical alterations observed in DMP1Cre,CαR mice. Since the number of osteocyte is much greater than the number of osteoblasts in the bone, osteocyte CαR was likely the major contributor.

Newly discovered targets of PKA have been identified, expanding the role of PKA in signal transduction. PKA phosphorylation of a histone lysine demethylase complex can activate the complex for subsequent epigenetic modulation and transcriptional regulation [69]. PKA pathway has also been shown to cross-talk with Wnt/β-catenin pathway [59,60]. Osteoblasts and osteocytes may express other as yet unidentified GPCRs that activate PKA. The present results highlight the role of PKA activity in osteocytes and late stage osteoblasts in skeletal homeostasis, and how this can be exploited for the development of novel anabolic therapies.

Conclusions

This study demonstrates that activation of the PKA pathway in osteocytes and late osteoblasts in vivo is sufficient for the initiation of an anabolic skeletal response. PKA in osteocytes and osteoblasts may function to integrate converging extracellular signals such as hormones and mechanical stimuli to produce an adaptive skeleton.

Supplementary Material

Refer to Web version on PubMed Central for supplementary material.

References

[1]. Quarles LD. FGF23, PHEX, and MEPE regulation of phosphate homeostasis and skeletal mineralization. Am J Physiol Endocrinol Metab. 2003; 285:E1–9. [PubMed: 12791601]

[2]. Feng JQ, Ward LM, Liu S, Lu Y, Xie Y, Yuan B, et al. Loss of DMP1 causes rickets and osteomalacia and identifies a role for osteocytes in mineral metabolism. Nat Genet. 2006; 38:1310–5. [PubMed: 17033621]

[3]. Lorenz-Depiereux B, Bastepe M, Benet-Pages A, Amyere M, Wagenstaller J, Muller-Barth U, et al. DMP1 mutations in autosomal recessive hypophosphatemia implicate a bone matrix protein in the regulation of phosphate homeostasis. Nat Genet. 2006; 38:1248–50. [PubMed: 17033625]

[4]. Zhao S, Zhang YK, Harris S, Ahuja SS, Bonewald LF. MLO-Y4 osteocyte-like cells support osteoclast formation and activation. J Bone Miner Res. 2002; 17:2068–79. [PubMed: 12412815]

[5]. Heino TJ, Hentunen TA, Vaananen HK. Osteocytes inhibit osteoclastic bone resorption through transforming growth factor-beta: enhancement by estrogen. J Cell Biochem. 2002; 85:185–97. [PubMed: 11891862]

[6]. van Bezooijen RL, Roelen BA, Visser A, van der Wee-Pals L, de Wilt E, Karperien M, et al. Sclerostin is an osteocyte-expressed negative regulator of bone formation, but not a classical BMP antagonist. J Exp Med. 2004; 199:805–14. [PubMed: 15024046]

[7]. Heino TJ, Hentunen TA, Vaananen HK. Conditioned medium from osteocytes stimulates the proliferation of bone marrow mesenchymal stem cells and their differentiation into osteoblasts. Exp Cell Res. 2004; 294:458–68. [PubMed: 15023534]

[8]. Gensure RC, Gardella TJ, Juppner H. Parathyroid hormone and parathyroid hormone-related peptide, and their receptors. Biochem Biophys Res Commun. 2005; 328:666–78. [PubMed: 15694400]

[9]. Juppner H, Abou-Samra AB, Freeman M, Kong XF, Schipani E, Richards J, et al. A G protein-linked receptor for parathyroid hormone and parathyroid hormone-related peptide. Science. 1991; 254:1024–6. [PubMed: 1658941]

[10]. Schwindinger WF, Fredericks J, Watkins L, Robinson H, Bathon JM, Pines M, et al. Coupling of the PTH/PTHrP receptor to multiple G-proteins. Direct demonstration of receptor activation of Gs, Gq/11, and Gi(1) by [alpha-32P]GTP-gammaazidoanilide photoaffinity labeling. Endocrine. 1998; 8:201–9. [PubMed: 9704578]

[11]. Ge C, Xiao G, Jiang D, Franceschi RT. Critical role of the extracellular signal–regulated kinase–MAPK pathway in osteoblast differentiation and skeletal development. J Cell Biol. 2007; 176:709–18. [PubMed: 17325210]

[12]. Rey A, Manen D, Rizzoli R, Caverzasio J, Ferrari SL. Proline-rich motifs in the parathyroid hormone (PTH)/PTH-related protein receptor C terminus mediate scaffolding of c-Src with beta-arrestin2 for ERK1/2 activation. J Biol Chem. 2006; 281:38181–8. [PubMed: 17038311]

[13]. Sakamoto A, Chen M, Nakamura T, Xie T, Karsenty G, Weinstein LS. Deficiency of the G-protein alpha-subunit G(s)alpha in osteoblasts leads to differential effects on trabecular and cortical bone. J Biol Chem. 2005; 280:21369–75. [PubMed: 15797856]

[14]. Hsiao EC, Boudignon BM, Chang WC, Bencsik M, Peng J, Nguyen TD, et al. Osteoblast expression of an engineered Gs-coupled receptor dramatically increases bone mass. Proc Natl Acad Sci U S A. 2008; 105:1209–14. [PubMed: 18212126]

[15]. Calvi LM, Sims NA, Hunzelman JL, Knight MC, Giovannetti A, Saxton JM, et al. Activated parathyroid hormone/parathyroid hormone-related protein receptor in osteoblastic cells differentially affects cortical and trabecular bone. J Clin Invest. 2001; 107:277–86. [PubMed: 11160151]

[16]. Peng JJ, Bencsik MM, Louie AA, Lu WW, Millard SS, Nguyen PP, et al. Conditional expression of a Gi-coupled receptor in osteoblasts results in trabecular osteopenia. Endocrinology. 2008; 149:1329–37. [PubMed: 18048501]

[17]. Millard SM, Louie AM, Wattanachanya L, Wronski TJ, Conklin BR, Nissenson RA. Blockade of receptor-activated G(i) signaling in osteoblasts in vivo leads to site-specific increases in cortical and cancellous bone formation. J Bone Miner Res. 2011; 26:822–32. [PubMed: 20939063]

[18]. Bruce JI, Straub SV, Yule DI. Crosstalk between cAMP and Ca^{2+} signaling in non-excitable cells. Cell Calcium. 2003; 34:431–44. [PubMed: 14572802]

[19]. Bos JL. Epac proteins: multi-purpose cAMP targets. Trends Biochem Sci. 2006; 31:680–6. [PubMed: 17084085]

[20]. Holz GG, Kang G, Harbeck M, Roe MW, Chepurny OG. Cell physiology of cAMP sensor Epac. J Physiol. 2006; 577:5–15. [PubMed: 16973695]

[21]. Fujita T, Meguro T, Fukuyama R, Nakamuta H, Koida M. New signaling pathway for parathyroid hormone and cyclic AMP action on extracellular-regulated kinase and cell proliferation in bone cells. Checkpoint of modulation by cyclic AMP. J Biol Chem. 2002; 277:22191–200. [PubMed: 11956184]

[22]. Fermor B, Skerry TM. PTH/PTHrP receptor expression on osteoblasts and osteocytes but not resorbing bone surfaces in growing rats. J Bone Miner Res. 1995; 10:1935–43. [PubMed: 8619374]

[23]. Davidovitch Z, Montgomery PC, Shanfeld JL. Cellular localization and concentration of bone cyclic nucleotides in response to acute PTE administration. Calcif Tissue Res. 1977; 24:81–91. [PubMed: 74278]

[24]. van der Plas A, Aarden EM, Feijen JH, de Boer AH, Wiltink A, Alblas MJ, et al. Characteristics and properties of osteocytes in culture. J Bone Miner Res. 1994; 9:1697–704. [PubMed: 7863820]

[25]. Bodine PV, Vernon SK, Komm BS. Establishment and hormonal regulation of a conditionally transformed preosteocytic cell line from adult human bone. Endocrinology. 1996; 137:4592–604. [PubMed: 8895322]

[26]. Kato Y, Windle JJ, Koop BA, Mundy GR, Bonewald LF. Establishment of an osteocyte-like cell line, MLO-Y4. J Bone Miner Res. 1997; 12:2014–23. [PubMed: 9421234]

[27]. Jilka RL, Weinstein RS, Bellido T, Roberson P, Parfitt AM, Manolagas SC. Increased bone formation by prevention of osteoblast apoptosis with parathyroid hormone. J Clin Invest. 1999; 104:439–46. [PubMed: 10449436]

[28]. Miyauchi A, Notoya K, Mikuni-Takagaki Y, Takagi Y, Goto M, Miki Y, et al. Parathyroid hormone-activated volume-sensitive calcium influx pathways in mechanically loaded osteocytes. J Biol Chem. 2000; 275:3335–42. [PubMed: 10652322]

[29]. Bringhurst FR. PTH receptors and apoptosis in osteocytes. J Musculoskelet Neuronal Interact. 2002; 2:245–51. [PubMed: 15758445]

[30]. O'Brien CA, Plotkin LI, Galli C, Goellner JJ, Gortazar AR, Allen MR, et al. Control of bone mass and remodeling by PTH receptor signaling in osteocytes. PLoS One. 2008; 3:e2942. [PubMed: 18698360]

[31]. Powell WF Jr, Barry KJ, Tulum I, Kobayashi T, Harris SE, Bringhurst FR, et al. Targeted ablation of the PTH/PTHrP receptor in osteocytes impairs bone structure and homeostatic calcemic responses. J Endocrinol. 2011; 209:21–32. [PubMed: 21220409]

[32]. Sakai A, Sakata T, Ikeda S, Uchida S, Okazaki R, Norimura T, et al. Intermittent administration of human parathyroid Hormone(1–34) prevents immobilization-related bone loss by regulating bone marrow capacity for bone cells in ddY mice. J Bone Miner Res. 1999; 14:1691–9. [PubMed: 10491216]

[33]. Kim CH, Takai E, Zhou H, von Stechow D, Muller R, Dempster DW, et al. Trabecular bone response to mechanical and parathyroid hormone stimulation: the role of mechanical microenvironment. J Bone Miner Res. 2003; 18:2116–25. [PubMed: 14672346]

[34]. Turner RT, Lotinun S, Hefferan TE, Morey-Holton E. Disuse in adult male rats attenuates the bone anabolic response to a therapeutic dose of parathyroid hormone. J Appl Physiol. 2006; 101:881–6. [PubMed: 16675609]

[35]. Zhou H, Iida-Klein A, Lu SS, Ducayen-Knowles M, Levine LR, Dempster DW, et al. Anabolic action of parathyroid hormone on cortical and cancellous bone differs between axial and appendicular skeletal sites in mice. Bone. 2003; 32:513–20. [PubMed: 12753867]

[36]. Conaway HH, Waite LC, Kenny AD. Immobilization and bone mass in rats. Effects of parathyroidectomy and acetazolamide. Calcif Tissue Res. 1973; 11:323–30. [PubMed: 4707199]

[37]. Lindgren JU. Studies of the calcium accretion rate of bone during immobilization in intact and thyroparathyroidectomized adult rats. Calcif Tissue Res. 1976; 22:41–7. [PubMed: 1000342]

[38]. Bellido T, Ali AA, Gubrij I, Plotkin LI, Fu Q, O'Brien CA, et al. Chronic elevation of parathyroid hormone in mice reduces expression of sclerostin by osteocytes: a novel mechanism for hormonal control of osteoblastogenesis. Endocrinology. 2005; 146:4577–83. [PubMed: 16081646]

[39]. Keller H, Kneissel M. SOST is a target gene for PTH in bone. Bone. 2005; 37:148–58. [PubMed: 15946907]

[40]. Cherian PP, Cheng B, Gu S, Sprague E, Bonewald LF, Jiang JX. Effects of mechanical strain on the function of Gap junctions in osteocytes are mediated through the prostaglandin EP2 receptor. J Biol Chem. 2003; 278:43146–56. [PubMed: 12939279]

[41]. Cherian PP, Siller-Jackson AJ, Gu S, Wang X, Bonewald LF, Sprague E, et al. Mechanical strain opens connexin 43 hemichannels in osteocytes: a novel mechanism for the release of prostaglandin. Mol Biol Cell. 2005; 16:3100–6. [PubMed: 15843434]

[42]. Kirschner LS, Carney JA, Pack SD, Taymans SE, Giatzakis C, Cho YS, et al. Mutations of the gene encoding the protein kinase A type I-alpha regulatory subunit in patients with the Carney complex. Nat Genet. 2000; 26:89–92. [PubMed: 10973256]

[43]. Cho-Chung YS, Nesterova M, Becker KG, Srivastava R, Park YG, Lee YN, et al. Dissecting the circuitry of protein kinase A and cAMP signaling in cancer genesis: antisense, microarray, gene overexpression, and transcription factor decoy. Ann N Y Acad Sci. 2002; 968:22–36. [PubMed: 12119265]

[44]. Miller WR. Regulatory subunits of PKA and breast cancer. Ann N Y Acad Sci. 2002; 968:37–48. [PubMed: 12119266]

[45]. Bonewald LF. Establishment and characterization of an osteocyte-like cell line, MLO-Y4. J Bone Miner Metab. 1999; 17:61–5. [PubMed: 10084404]

[46]. Kato Y, Boskey A, Spevak L, Dallas M, Hori M, Bonewald LF. Establishment of an osteoid preosteocyte-like cell MLO-A5 that spontaneously mineralizes in culture. J Bone Miner Res. 2001; 16:1622–33. [PubMed: 11547831]

[47]. Toyosawa S, Shintani S, Fujiwara T, Ooshima T, Sato A, Ijuhin N, et al. Dentin matrix protein 1 is predominantly expressed in chicken and rat osteocytes but not in osteoblasts. J Bone Miner Res. 2001; 16:2017–26. [PubMed: 11697797]

[48]. Lu Y, Zhang S, Xie Y, Pi Y, Feng JQ. Differential regulation of dentin matrix protein 1 expression during odontogenesis. Cells Tissues Organs. 2005; 181:241–7. [PubMed: 16612089]

[49]. Lu Y, Xie Y, Zhang S, Dusevich V, Bonewald LF, Feng JQ. DMP1-targeted Cre expression in odontoblasts and osteocytes. J Dent Res. 2007; 86:320–5. [PubMed: 17384025]

[50]. Orellana SA, McKnight GS. Mutations in the catalytic subunit of cAMP-dependent protein kinase result in unregulated biological activity. Proc Natl Acad Sci U S A. 1992; 89:4726–30. [PubMed: 1584809]

[51]. Niswender CM, Willis BS, Wallen A, Sweet IR, Jetton TL, Thompson BR, et al. Cre recombinase-dependent expression of a constitutively active mutant allele of the catalytic subunit of protein kinase A. Genesis. 2005; 43:109–19. [PubMed: 16155866]

[52]. Howe DG, Clarke CM, Yan H, Willis BS, Schneider DA, McKnight GS, et al. Inhibition of protein kinase A in murine enteric neurons causes lethal intestinal pseudo-obstruction. J Neurobiol. 2006; 66:256–72. [PubMed: 16329126]

[53]. Gibson RM, Taylor SS. Dissecting the cooperative reassociation of the regulatory and catalytic subunits of cAMP-dependent protein kinase. Role of Trp-196 in the catalytic subunit. J Biol Chem. 1997; 272:31998–2005. [PubMed: 9405392]

[54]. Xiong JOM, Cazer P, Chen X, Weinstein R, Jilka R, Manolagas S, et al. Hypertrophic chondrocytes and osteocytes are essential sources of RANKL for bone growth and for bone remodeling, respectively. J Bone Miner Res. 2010; 25(Suppl. 1) [Available at http://www.asbmr.org/Meetings/AnnualMeeting/AbstractDetail.aspx?aid=07071c f2-edc3-4c53-96db-d9d18203f82c].

[55]. Gong Y, Slee RB, Fukai N, Rawadi G, Roman-Roman S, Reginato AM, et al. LDL receptor-related protein 5 (LRP5) affects bone accrual and eye development. Cell. 2001; 107:513–23. [PubMed: 11719191]

[56]. Boyden LM, Mao J, Belsky J, Mitzner L, Farhi A, Mitnick MA, et al. High bone density due to a mutation in LDL-receptor-related protein 5. N Engl J Med. 2002; 346:1513–21. [PubMed: 12015390]

[57]. Little RD, Carulli JP, Del Mastro RG, Dupuis J, Osborne M, Folz C, et al. A mutation in the LDL receptor-related protein 5 gene results in the autosomal dominant high-bone-mass trait. Am J Hum Genet. 2002; 70:11–9. [PubMed: 11741193]

[58]. Rhee Y, Allen MR, Condon K, Lezcano V, Ronda AC, Galli C, et al. PTH receptor signaling in osteocytes governs periosteal bone formation and intracortical remodeling. J Bone Miner Res. 2011; 26:1035–46. [PubMed: 21140374]

[59]. Hino S, Tanji C, Nakayama KI, Kikuchi A. Phosphorylation of beta-catenin by cyclic AMP-dependent protein kinase stabilizes beta-catenin through inhibition of its ubiquitination. Mol Cell Biol. 2005; 25:9063–72. [PubMed: 16199882]

[60]. Suzuki A, Ozono K, Kubota T, Kondou H, Tachikawa K, Michigami T. PTH/cAMP/PKA signaling facilitates canonical Wnt signaling via inactivation of glycogen synthase kinase-3beta in osteoblastic Saos-2 cells. J Cell Biochem. 2008; 104:304–17. [PubMed: 17990294]

[61]. O'Brien C, Plotkin L, Vyas K, Cazer P, Gortazar A, Goellner J, et al. Activation of PTH receptor 1 specifically in osteocytes suppresses SOST expression and increases bone mass in transgenic mice. J Bone Miner Res. 2006:S4.

[62]. Rhee Y, Allen MR, Condon K, Lezcano V, Ronda AC, Galli C, et al. PTH receptor signaling in osteocytes governs periosteal bone formation and intracortical remodeling. J Bone Miner Res. 2011; 26:1035–46. [PubMed: 21140374]

[63]. Powell WF Jr, Barry KJ, Tulum I, Kobayashi T, Harris SE, Bringhurst FR, et al. Targeted ablation of the PTH/PTHrP receptor in osteocytes impairs bone structure and homeostatic calcemic responses. J Endocrinol. 2011; 209:21–32. [PubMed: 21220409]

[64]. Robling AG, Niziolek PJ, Baldridge LA, Condon KW, Allen MR, Alam I, et al. Mechanical stimulation of bone in vivo reduces osteocyte expression of SOST/sclerostin. J Biol Chem. 2008; 283:5866–75. [PubMed: 18089564]

[65]. Lin C, Jiang X, Dai Z, Guo X, Weng T, Wang J, et al. Sclerostin mediates bone response to mechanical unloading through antagonizing Wnt/beta-catenin signaling. J Bone Miner Res. 2009; 24:1651–61. [PubMed: 19419300]

[66]. Tatsumi S, Ishii K, Amizuka N, Li M, Kobayashi T, Kohno K, et al. Targeted ablation of osteocytes induces osteoporosis with defective mechanotransduction. Cell Metab. 2007; 5:464–75. [PubMed: 17550781]

[67]. Akhter MP, Wells DJ, Short SJ, Cullen DM, Johnson ML, Haynatzki GR, et al. Bone biomechanical properties in LRP5 mutant mice. Bone. 2004; 35:162–9. [PubMed: 15207752]

[68]. Kitase Y, Barragan L, Qing H, Kondoh S, Jiang JX, Johnson ML, et al. Mechanical induction of PGE2 in osteocytes blocks glucocorticoid-induced apoptosis through both the beta-catenin and PKA pathways. J Bone Miner Res. 2010; 25:2657–68. [PubMed: 20578217]

[69]. Backs J, Worst BC, Lehmann LH, Patrick DM, Jebessa Z, Kreusser MM, et al. Selective repression of MEF2 activity by PKA-dependent proteolysis of HDAC4. J Cell Biol. 2011; 195:403–15. [PubMed: 22042619]

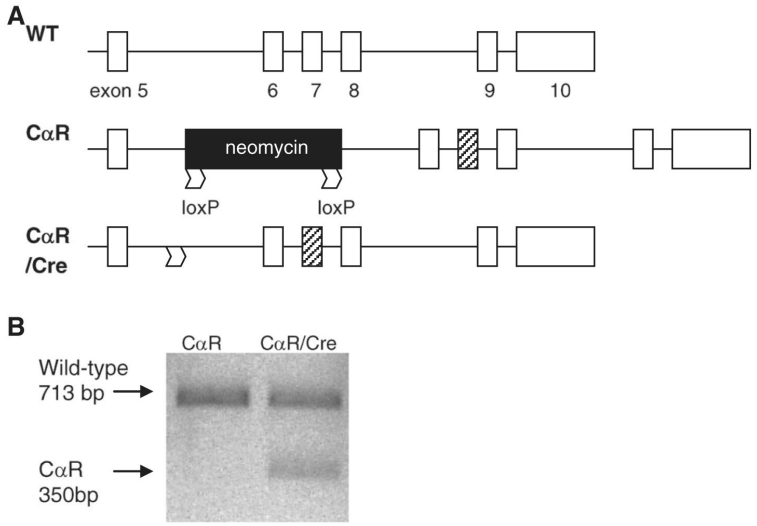

Fig. 1.

Expression of Cre induces CαR transcription. (A)CαR has a W196R mutation within exon 7 (black box). “Silent” CαR contains an intervening floxed neomycin cassette between exons 5 and 6, preventing production of full CαR transcript. In the presence of Cre recombinase, Cre recognizes loxP sites and excises the neomycin cassette and permits production of CαR transcript. Abbreviation: WT = wild-type. (B) To detect CαR transcript, PCR fragments were amplified using primers within exons 3 and 10 of Cα cDNA (forward 5′-GGTGGTGAAGCTAAAGCA-3′ and reverse 5′-GGTATGAAGGGAGCTTCC-3′), followed by *Mlu I* digestion, resulted in a 713 bp fragment corresponding to wild-type mRNA versus fragments of 350 and 363 bp if the PCR product contained the CαR mutation. The PCR fragments were resolved on a 1% agarose gel and visualized with SBYR Green Safe DNA gel stain. Because the mice were heterozygous for CαR, cells isolated from them expressed one copy of wild-type Cα. As a result, the 713 bp fragment representing the wild-type mRNA was always detected.

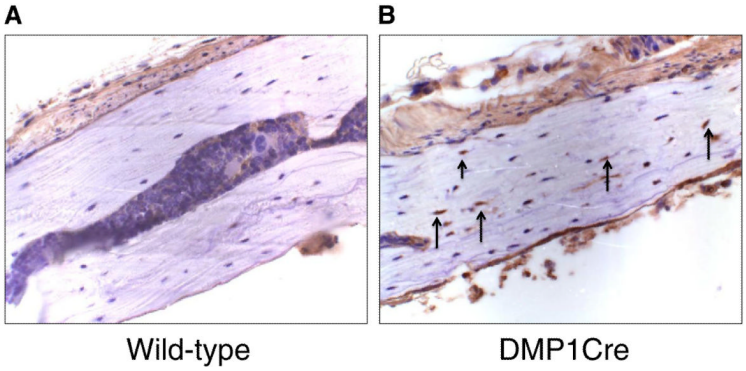

Fig. 2.

DMP1 directs the expression of Cre in osteocytes. Immunohistochemistry using an antibody against Cre recombinase failed to detect the expression of Cre in osteocytes in the female wild-type calvarial sagittal section (A). Cre expression was detected in the female single transgenic DMP1Cre calvarial section, as indicated by arrows (B).

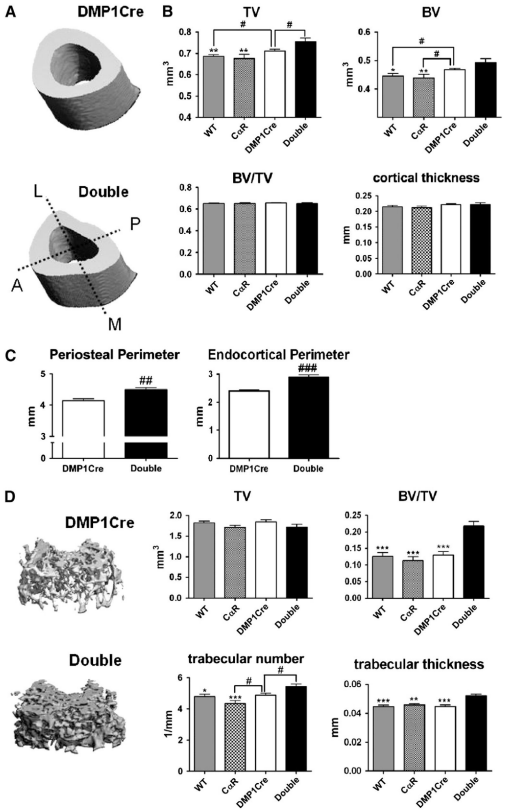

Fig. 3.

Constitutively active PKA signaling in osteocytes and late osteoblasts alters cortical bone shape proximal to TFJ and increases trabecular bone in the distal femur. (A) Representative three-dimensional reconstruction images of cortical bone 40-microns proximal to TFJ. (B) Cortical bone parameters of all four genotypes as determined by μCT. (C) Periosteal and endocortical perimeters of cortical bone as determined by histomorphometry. (D) Trabecular bone parameters as determined by μCT. All data are mean ± SEM and collected from 3-month old female mice ($n \geq 10$ per genotype). 1-way ANOVA Bonferroni all pairs: * $p < 0.05$, ** $p < 0.01$, *** $p < 0.001$. *T*-test: # $p < 0.05$. Abbreviation: TV = tissue volume, BV =bone volume, Double = double transgenic (DMP1Cre,CαR).

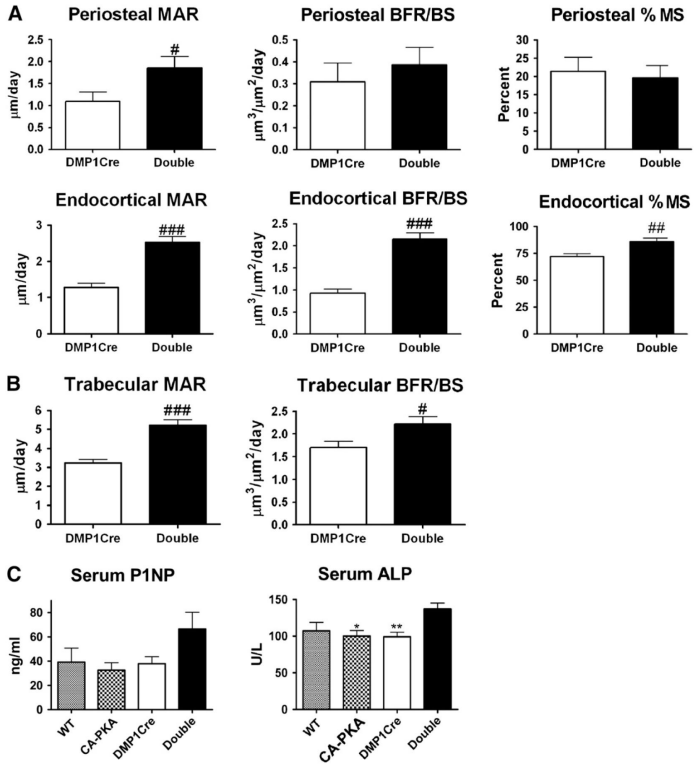

Fig. 4.

Constitutively active PKA signaling in osteocytes and late osteoblasts increases bone formation. (A) Dynamic histomorphometric measurements of cortical bone surfaces in the cortical bone proximal to TFJ ($n \geq 7$). (B) Dynamic histomorphometric measurements of the trabecular bone surface ($n = 7$). (C) Serum propeptide of type 1 collagen (P1NP) and alkaline phosphatase (ALP) levels ($n \geq 6$). All data are mean ± SEM and collected from 3-month old female mice. 1-way ANOVA Bonferroni all pairs: * $p < 0.05$, ** $p < 0.01$. *T*-test: # $p < 0.05$, ### $p < 0.001$. Abbreviation: MAR = mineral apposition rate, BFR/BS = bone formation rate/bone surface, MS = mineralizing surface.

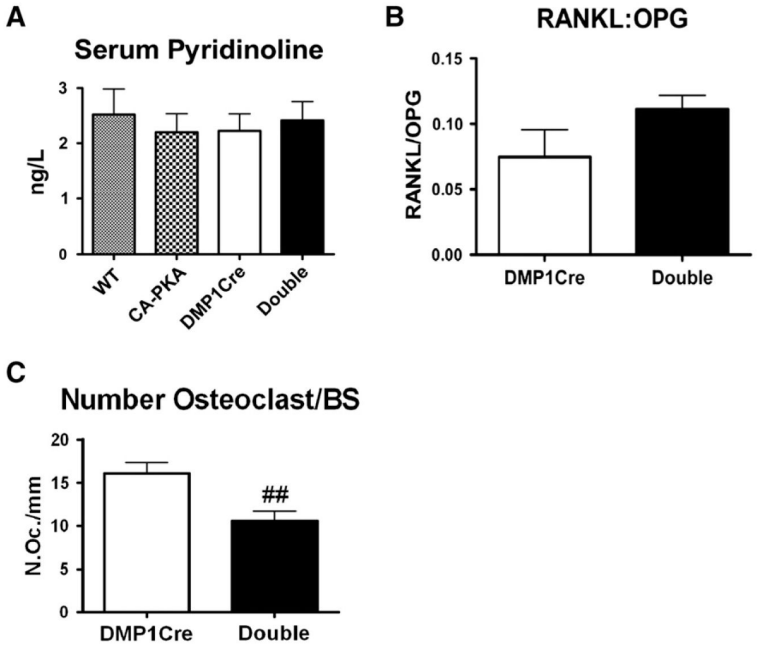

Fig. 5.

DMP1Cre,CαR mice exhibit no detectable increases in bone resorption. (A) Serum pyridinoline ($n \geq 7$). (B) Ratio of the transcript levels of RANKL:OPG, relative to L19 expression, in the long bone RNA ($n \geq 4$). (C) Histomorphometric measurement of osteoclast number per bone surface in the trabecular bone ($n = 7$). All data are mean ± SEM and collected from 3-month female mice. *T*-test: ## $p < 0.01$. Abbreviation: BS = bone surface.

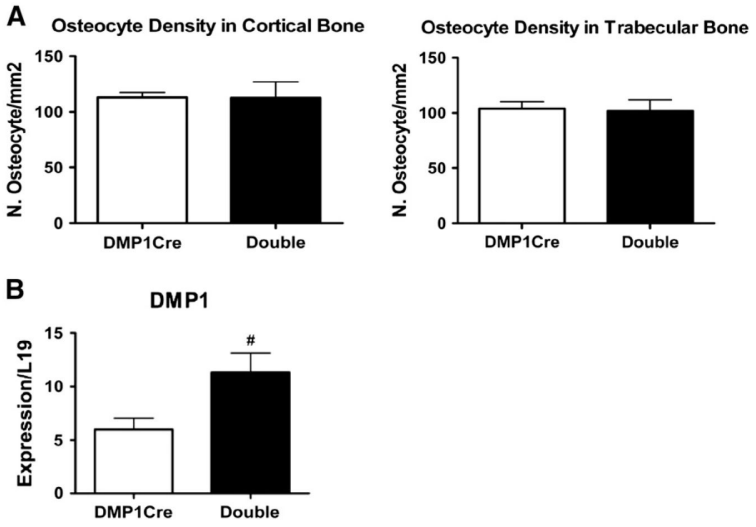

Fig. 6.

Constitutively active PKA signaling in osteocytes does not alter osteocyte density but whole bone DMP1 transcript levels are up-regulated. (A) Histomorphometric measurements of osteocyte density in the cortical and trabecular bones in the distal femur ($n \geq 5$). (B) Real-time PCR detection for DMP1 transcript levels in the long bone RNA, normalized to L19. All data are mean ± SEM and collected from 3-month old female mice. *T*-test: # $p < 0.05$. Double = double transgenic (DMP1Cre,Cα*R*).

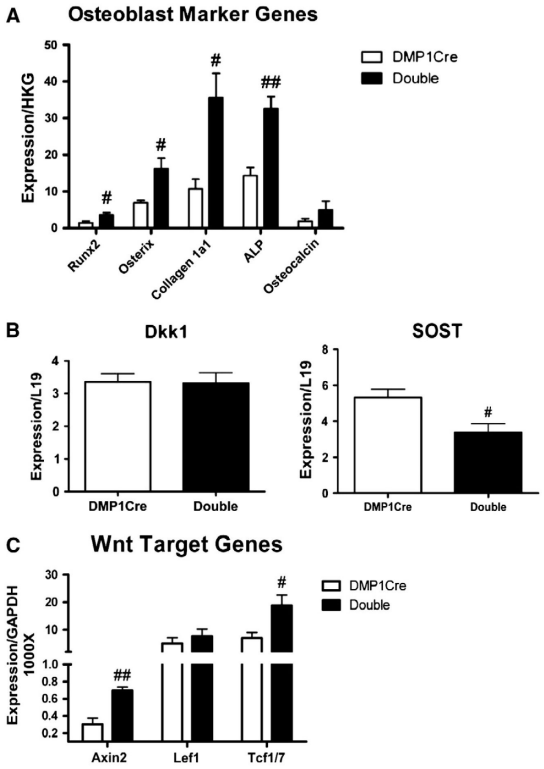

Fig. 7.

In the long bones of DMP1Cre,CαR mice, genes associated with osteoblast differentiation are up-regulated while SOST expression is down-regulated. (A) Real-time PCR analysis of genes that are associated with osteoblast differentiation, (B) encode for negative regulators of Wnt signaling, and (C) targets of canonical Wnt pathway. RNA was extracted from the whole bone of femurs and tibiae. HKG denotes housekeeping genes. Runx2, osterix, and ALP expression are normalized to L19. Collagen 1α1 and osteocalcin are normalized to GAPDH. All data are mean ± SEM and collected from 3-month old female mice. n ≥ 4. *T*-test: # $p < 0.05$, ## $p < 0.01$.